MODELLING AND OBSERVING THE 8.8 CHILE AND 9.0 JAPAN EARTHQUAKES USING GOCE

T. Broerse[1], P. Visser[1], J. Bouman[2], M. Fuchs[2], B. Vermeersen[1], and M. Schmidt[2]

[1]*Faculty of Aerospace Engineering, Delft University of Technology, Kluyverweg 1 2629 HS Delft, The Netherlands*
[2]*Deutsches Geodätisches Forschungsinstitut, Alfons-Goppel-Str. 11, 80539 München, Germany*

ABSTRACT

Large earthquakes do not only heavily deform the crust in the vicinity of the fault, they also change the gravity field of the area affected by the earthquake due to mass redistribution in the upper layers of the Earth. Besides that, for sub-oceanic earthquakes deformation of the ocean floor causes relative sea-level changes and mass redistribution of water that has again a significant effect on the gravity field. Such a sub-oceanic earthquake occurred on 27 February 2010 in central Chili with a magnitude of Mw 8.8 and on 11 March 2011 with a magnitude of Mw 9.0 near the east coast of Honshu, Japan. This makes both a potential candidate for detecting the co-seismic gravity changes in the GOCE gradiometer data. We will assess the detectability of gravity field changes in the GOCE gravity gradients by modelling these earthquakes using a forward model as well as taking differences of GOCE data before and after the respective earthquakes.

Key words: GOCE; Chile 8.8 earthquake; Japan 9.0 earthquake; time variable gravity.

1. INTRODUCTION

While the GOCE mission is designed for mapping the Earth's stationary gravity field we think that it is worthwhile studying the presence of time-variable signals in GOCE's gravity gradient observations. Because of the extended operational lifetime, beyond its original 20-month design lifetime, it might be possible to extract trends or sudden changes in the gravity field from the GOCE observations. Next, the occurrence of two very heavy earthquakes within the observational period of GOCE give us the opportunity to test whether GOCE is capable of detecting quasi-stepsize changes in gravity gradients or derivative gravity fields.

The large and catastrophic 9.1 magnitude Sumatra-Andaman earthquake from 26 December 2004 led to many studies that investigated the co-seismic changes in the gravity field as detected by that other important gravity mission, GRACE (Han et al., 2006; Chen et al., 2007; Panet et al., 2007; Han and Simons, 2008; de Linage et al., 2009; Broerse et al., 2011). According to these studies GRACE has indeed been able to identify the long wavelength features of the co-seismic, and even post-seismic, changes that were caused by internal mass displacement of the solid earth due the slip on the approximate 1500 km long fault. As de Linage et al. (2009) and Broerse et al. (2011) pointed out, the displacement of ocean water due to changes in bathymetry led to significant secondary changes in the co-seismic gravity field that are needed to match GRACE observations with earthquake gravity models. Since other geodetic observations such as GPS, InSAR or in-situ observations of uplift seen from coral reefs do only constrain the size and location of sub-oceanic earthquakes from land, gravity observations serve as additional independent measurements that indicate the total mass displacement related to large thrust earthquakes.

Allthough GOCE was not operational at the time of the 2004 Sumatra-Andaman earthquake, it has been measuring gravity gradients at the occurrence of the 8.8 earthquake of 27 February 2010 in Chile and the 9.0 earthquake of 11 March 2011 near the coast of Japan. With respect to GRACE it conducts 3D measurements instead of 1D and is sensitive to smaller wavelength signals than GRACE. Vertical deformation, and related gravity field changes, have still a high signal strength at resolutions smaller than what is visible with GRACE, which is measured up to a resolution of roughly 400 km (Tapley et al., 2004). Also GOCE might fill this gap and could prove to give additional information on earthquake mechanisms. This study is in that view a test case for GOCE.

In this paper we present our ongoing research that connects forward models of co-seismic gravity changes to an analysis of GOCE gravity gradients. While both the 8.8 Chile earthquake and 9.0 Japan earthquake have led to numerous casualties and many people lost houses and properties, at the same time these earthquakes provide geophysicists a laboratory to better understand earthquake mechanisms. In the following sections we will first quickly review finished and ongoing gravity research to both earthquakes. After this we will outline our forward models that we use to predict the earthquake

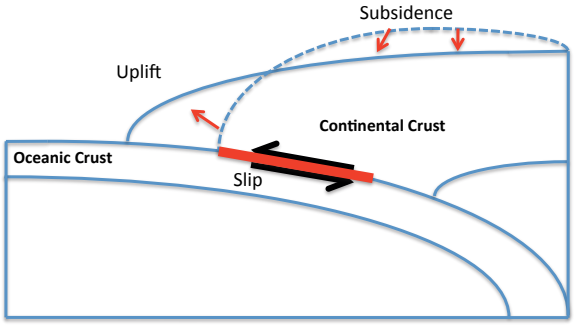

Figure 1. A simplified model for the co-seismic elasic deformation. Dashed lines denote the pre-seismic surface. Due to slip on the interface between oceanic and continental crust, built up stresses are released and the continental is allowed to deform back to its unstressed form.

signal that GOCE should be measuring. Subsequently we present (preliminary) results in terms of change in geoid height and gravity gradients at GOCE height. Then, we briefly discuss parameters for optimally filtering GOCE gravity gradient data in order to test whether co-seismic signals are observable in the data. We finalise by making a few conclusions.

2. STATE OF ART CO-SEISMIC GRAVITY RESEARCH

As we already mentioned in the introduction the massive 2004 Sumatra-Andaman earthquake was the first earthquake for which a change in gravity field could be measured from space. A series of papers has since been published that showed that GRACE was indeed capable of discerning the co-seismic gravity signal (Han et al., 2006; Chen et al., 2007; Panet et al., 2007; Han and Simons, 2008; de Linage et al., 2009; Broerse et al., 2011). While the 8.8 Chile earthquake was smaller in magnitude and the slip was confined to a smaller area, both Han et al. (2010) and Heki and Matsuo (2010) showed that GRACE probably detected the long wavelength part of the gravity signal of this earthquake. Here Heki and Matsuo (2010) model and detect a gravity jump up to -5 μGal, truncated at a spherical harmonic degree 60 and smoothed at a 300 km smoothing radius. The USGS estimated a magnitude 9.0 earthquake near the east coast of Honshu, Japan (USGS, 2011), which makes us presume that the gravity change signal will be larger than that of the Chile earthquake. Since the Japan earthquake is very recent, slip inversions for this earthquake are still being prepared, but first non-reviewed slip inversions are already available online by various research groups. At the time of writing no publications on gravity changes based on GRACE have been published yet for the Japan earthquake.

3. OUR FORWARD MODELS

To forward model the solid earth responses to the seismic slip: deformations and associated gravity changes, we use a semi-analytic normal mode model where the earth is represented as a spherically multi-layered and self-gravitating body with a compressible elastic rheology (Sabadini and Vermeersen, 2004). We determine sea-level changes and resulting gravity field perturbations using an adapted version of the sea-level equation (SLE) that has been used for Glacial Isostatic Adjustment studies, first by Farrell and Clark (1976). The sea-level equation, next to our normal mode model for seismic solid earth modeling, allows us to predict a gravitationally self-consistent solution for the co-seismic relative sea-level, surface deformation and gravity field changes. Model results are used to construct 3-D gradients at GOCE altitude that will be compared to gravity gradient differences before and after the earthquake.

In figure 1 is shown how for shallow earthquakes - this applies to both the 8.8 Chile and 9.0 Japan earthquake - uplift and subsidence is expected once the friction at the interface between subsiding oceanic crust and lithosphere and continental crust and lithosphere is overcome by built up stresses. These stresses are due to (partly) opposite tectonic velocities and are being released when the earthquake happens. For gravity modelling the vertical deformation is important since this implies mass redistribution. The vertical deformation is mainly caused by the slip in dip direction and for a thrust earthquake it is expected that uplift occurs close to where the fault intersects with the surface and subsidence occurs further away from the fault, which is usually land inwards. The figure is a highly simplified representation and our solid earth model solves for the deformation due to a dislocation in the earth much more detailed in an analytic way. But nontheless figure 1 serves as a good tool for understanding the physical mechanism.

As we already mentioned, our model consists of a solid earth model that approximates deformation and gravity field changes due to seismic slip, but we model the contribution of the ocean to deformation and the gravity field as well. The ocean model, a seismic version of the sea-level equation (SLE), is based on the pseudo-spectral algorithm for solving the SLE by Mitrovica and Peltier (1991). The adaption for the seismic case has been published in our recent paper where we apply the method to the Sumatra-Andaman earthquake. Here we show how the combination of the ocean response to a large scale uplift of the sea floor leads to a geoid height change that, combined with the solid earth gravity field change, agrees well with GRACE observations (Broerse et al., 2011). In figure 2 we point out how the presence of an ocean diminishes the gravity signal by solid earth deformation at those locations where there is no land. The SLE discriminates between sea and land covered areas, which is important for both the Chile and Japan earthquake as both happened along the ocean-continental boundary.

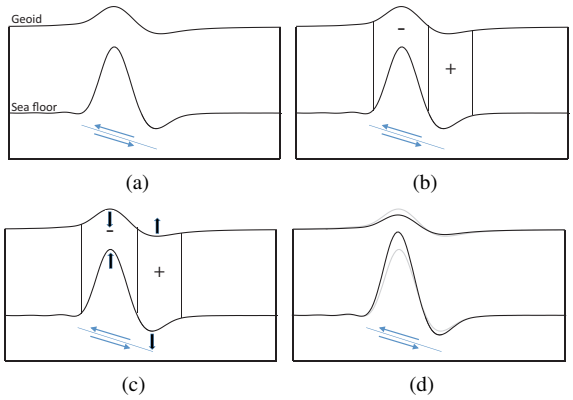

Figure 2. The principle behind the ocean response to the direct solid earth deformation and geoid change due to seismic slip. The fault in this example typically has a dip angle around 15 ° and starts at the left top and dips to the right. (a) Vertical deformation of the sea floor and geoid height change caused by the solid earth model. (b) Because the vertical deformation of the sea floor is typically two orders of magnitude larger than the geoid height change, we expect a relative sea level fall at the left and a relative sea level rise at the right. (c) Because of the smaller water column at the left, the load on the sea floor is smaller and we expect extra uplift of the sea floor and a decrease in geoid height since the ocean locally contains less mass. At the right there is a larger water column, meaning extra subsidence because of an increased load and increase in geoid height due to extra water mass. (d) The combined effect of the direct co-seismic solid earth responses and ocean water redistribution on vertical deformation and geoid height change. The solid earth only responses are denoted in grey, the combined solid earth and ocean effects are shown in black. With respect to the solid earth only result we expect an increase in the vertical deformation due to the presence of an ocean and a diminishing effect on geoid height.

The input for our normal mode model is a slip model that describes the location, strength and direction of the slip. For the Chile case we used the slip inversion of Delouis et al. (2010) that uses GPS, InSAR and broadband teleseismic data as input. In this model the slip is estimated as an elongated rupture with two main slip zones, or asperities. In these two asperities slip up to 13 m and 21 m is reached. No slip distributions have been published yet in peer-reviewed journals for the 9.0 Japan earthquake. Therefore we used the GFZ fault slip model published online by Wang and Walter (2011). The rheology used is compressible and elastic; properties of the solid earth are derived from PREM (Dziewonski and Anderson, 1981). We compute the vertical deformation and geoid height change up to order and degree 450. Since at higher degrees and orders, for a complete fault, we lose less than 5% in terms of maximum amplitude this still gives a realistic approximation. In the following we present the preliminary results for changes in geoid height and gravity gradients at GOCE height.

4. FORWARD MODEL RESULTS

These are the preliminary results of the forward modelling which should give a good indication of the patterns of co-seismic change in the gravity field in terms of geoid height and gravity gradients as well as the signal strength. Starting with the Chile earthquake, in figure 3 we show the vertical deformation and geoid height change as direct solid earth response to the seismic slip, contribution of the ocean and the combined effect of solid earth and ocean respectively. Starting with the vertical deformation: the modelled direct effect of seismic slip on vertical deformation ranges between -2.6 and 3.9 m. It has the shape of an elongated dipole, with uplift just in front of the coastline and subsidence land inwards. The elastic deformation due to changed ocean load has a comparable pattern in the ocean area but is very small and ranges between 0 and 22 mm, which makes the combined effect of solid earth basically identical to the direct solid earth effect. Considering the change in geoid height, we see a comparable dipole as for the vertical deformation, but smaller in amplitude and more smooth. The direct solid earth effect of the seismic slip ranges between -8 and 16 mm. The effect of ocean mass redistribution driven by bathymetry changes is everywhere negative since the ocean floor only experiences uplift. A small wavelength part is visible which resembles the short wavelength uplift, however we can also see a relatively large long wavelength negative geoid anomaly which is driven by long wavelength uplift of the sea floor. The ocean effect ranges between -8 and 0 mm and combined with the solid earth geoid anomalies the total modelled geoid height change is between -11 and 9 mm. It can be observed that the inclusion of the ocean makes the co-seismic geoid height change more negative with respect to the solid earth model results. Since the area where the uplift is largest is below sea level and the area with the largest subsidence is located on land, the negative ocean effect is even larger than when there is also subsidence below sea level as we will see later on for the forward model for the Japan earthquake.

Next, the geoid height changes are converted to gravity gradients as they would have been measured along the GOCE orbit. The geoid height signal up to degree and order 450 is used in these calculations. In figure 4 these gravity gradients are displayed for the V_{XX}, V_{YY}, V_{ZZ} and V_{XZ} components for a period of 20 days. Because of the orbit height the gradients are more smoothed than the geoid height change, but at least in the V_{XX}, V_{YY} and V_{ZZ} the dipole signal is clearly visible. The V_{XZ} component looks slightly different because of different signs in ascending and descending orbits. Ranges in mEU between -0.07/0.12 for V_{XX}; -0.17/0.20 for V_{YY}; -0.31/0.20 for V_{ZZ}; and -0.12/0.16 for V_{XZ} are computed based on the forward modelling.

A comparable overview for the vertical deformation for the 9.0 Japan earthquake is given in figure 5. Geoid height change and vertical deformation are preliminary results since they are based on still unpublished slip

distributions. Our model results for both responses can still change when updates for the slip inversions become available. For the vertical deformation the direct solid earth effect is between -3.0 and 6.7 m. Comparable for the Chile earthquake, the expected ocean effect on vertical deformation is very small, between -7 and 42 mm. This results in a combined vertical deformation between -3.0 and 6.7 m. Again we modelled a dipole, but less elongated with respect to the Chile earthquake as the slip is thought to be more concentrated. The maximum changes for the geoid height change are larger than for the Chile earthquake, which can be expected due to its larger magnitude. Solid earth only effect on geoid height is between -13 and 31 mm. The ocean effect is slightly different than the previous case since the slip is located farther away from the coast, meaning a part of the subsidence is below sea level, partly compensating for the uplift in terms of ocean contribution to geoid height change. The ocean effect on the geoid ranges from -15 to 1 mm which makes the total effect between -12 and 16 mm. While the spatial extent of the geoid height change is smaller than that of the 2004 Sumatra-Andaman earthquake, it actually seems to be comparable in terms of maximum amplitude (Broerse et al., 2011).

In figure 6 the gravity gradients are displaced as modelled for the Japan 9.0 earthquake. As could already be expected from the larger magnitude and larger modelled geoid height change, we see a higher signal in the gravity gradients than for the Chile earthquake. Because the slip for the Japan earthquake is more localised around one asperity, and not spread out over an elongated rupture as for the Chile earthquake, the broader and smoother geoid height change leads to V_{YY} and V_{ZZ} gravity gradient components that are still quite strong at GOCE altitude. Ranges in mEU between -0.20/0.21 for V_{XX}; -0.46/0.36 for V_{YY}; -0.52/0.59 for V_{ZZ}; and -0.30/0.18 for V_{XZ} are computed.

5. GRAVITY GRADIENT ANALYSIS

Gravity gradients before and after both earthquakes will be analysed and compared. Next, we construct a local gravity model based on all gravity gradients. At the time of the GOCE user workshop this is still a work in progress and we are currently studying the effects of the binning sizes, the filter settings in the GOCE measurement bandwidth, time windows and the reference gravity field. In table 1 the standard deviations (σ) that we found for the most important gravity gradients are given. To reach a σ = 0.1 mEU in 2° grid cells between 0.3 and 2.3 GOCE repeat cycles are required, depending on the gradient, see table 2.

6. DISCUSSION AND CONCLUSIONS

To investigate what signal is expected in terms of gravity gradients at GOCE height from both the 8.8 Chile and 9.0 Japan earthquakes we applied forward models based on a solid earth model and a SLE model that computes the ocean response for geoid height change. Taking into account realistic slip distributions we found that the largest co-seismic signal in the GOCE gravity gradients is roughly between -0.31/0.20 mEU for the V_{ZZ} and -0.17/0.20 mEU for the V_{YY} gradient in the Chile case. This is well below the noise level for instantaneous gravity gradient measurements. Averaging over time and space will be needed to detect the seismic signal in the GOCE observations. At the moment of the GOCE user workshop we are not able to already indicate whether it is possible to identify the Chile earthquake gravity signature. However, for the Chile earthquake, it is a disadvantage that we only have roughly 2.5 months of data before the earthquake, limiting the possibilities for pre-seismic time averaging. In this respect the chances of being able to see the Japan 9.0 earthquake are higher, both due to the availability of observations multiple months before the earthquake epoch and the expected higher signal in the gravity gradients at GOCE orbit height. The highest ranges in gravity gradients for the 9.0 Japan earthquake are modelled for V_{YY}: between -0.46/0.36 mEU, and for V_{ZZ}: between -0.52/0.59 mEU. As the analysis of gradient data is currently in progress we expect more definite results of the gravity gradient analysis in the coming months. If GOCE is indeed able to see very large thrust earthquakes this will prove to be valuable information on the total mass displacement by such earthquakes. Not only GOCE might assist GRACE gravity research, it can also complement GRACE in those smaller wavelengths where earthquakes have still a large part of their gravity signal but that GRACE is not able to see.

Table 1. Gravity gradient σ in 1° grid cells $[mEU]$ for one repeat cycle

V_{XX}	V_{YY}	V_{ZZ}	V_{XZ}
1.4	1.1	2.6	2.7

Table 2. Required repeat cycles to reach $\sigma = 0.1$ in 2° grid cells $[mEU]$

V_{XX}	V_{YY}	V_{ZZ}	V_{XZ}
0.6	0.3	2.1	2.3

7. ACKNOWLEDGEMENTS

This study is sponsored by the ESA Support To Science Element. Furthermore Taco Broerse acknowledges financial support from ISES.

REFERENCES

Broerse, D., Vermeersen, L., Riva, R., and van der Wal, W. (2011). Ocean contribution to co-seismic crustal deformation and geoid anomalies: Application to the 2004 December 26 Sumatra-Andaman earthquake. *Earth Planet. Sci. Lett.*, In Press. doi:10.1016/j.epsl.2011.03.011.

Chen, J., Wilson, C., Tapley, B., and Grand, S. (2007). GRACE detects coseismic and postseismic deformation from the Sumatra-Andaman earthquake. *Geophys. Res. Lett.*, 34:L13302.

de Linage, C., Rivera, L., Hinderer, J., Boy, J., Rogister, Y., Lambotte, S., and Biancale, R. (2009). Separation of coseismic and postseismic gravity changes for the 2004 Sumatra–Andaman earthquake from 4.6 yr of GRACE observations and modelling of the coseismic change by normal-modes summation. *Geophys. J. Int.*, 176(3):695–714.

Delouis, B., Nocquet, J., and Vallée, M. (2010). Slip distribution of the February 27, 2010 Mw= 8.8 Maule Earthquake, central Chile, from static and high-rate GPS, InSAR, and broadband teleseismic data. *Geophys. Res. Lett.*, 37(17):L17305.

Dziewonski, A. and Anderson, D. (1981). Preliminary reference Earth model. *Phys. Earth Planet. Inter.*, 25(4):297–356.

Farrell, W. and Clark, J. (1976). On postglacial sea level. *Geophys. J. Int.*, 46:647–667.

Han, S., Sauber, J., and Luthcke, S. (2010). Regional gravity decrease after the 2010 Maule (Chile) earthquake indicates large-scale mass redistribution. *Geophys. Res. Lett.*, 37.

Han, S., Shum, C., Bevis, M., Ji, C., and Kuo, C. (2006). Crustal dilatation observed by GRACE after the 2004 Sumatra-Andaman earthquake. *Science*, 313(5787):658–662.

Han, S. and Simons, F. (2008). Spatiospectral localization of global geopotential fields from the Gravity Recovery and Climate Experiment (GRACE) reveals the coseismic gravity change owing to the 2004 Sumatra-Andaman earthquake. *J. Geophys. Res.*, 113(B1):B01405.

Heki, K. and Matsuo, K. (2010). Coseismic gravity changes of the 2010 earthquake in central Chile from satellite gravimetry. *Geophys. Res. Lett*, 37.

Mitrovica, J. and Peltier, W. (1991). On postglacial geoid subsidence over the equatorial oceans. *J. Geophys. Res.*, 96(B12):20053–20071.

Panet, I., Mikhailov, V., Diament, M., Pollitz, F., King, G., de Viron, O., Holschneider, M., Biancale, R., and Lemoine, J. (2007). Coseismic and post-seismic signatures of the Sumatra 2004 December and 2005 March earthquakes in GRACE satellite gravity. *Geophys. J. Int.*, 171(1):177–190.

Sabadini, R. and Vermeersen, B. (2004). *Global Dynamics of the Earth: Applications of Normal Mode Relaxation Theory to Solid-Earth Geophysics*. Kluwer Acad. Publ., Dordrecht, Netherlands.

Tapley, B., Bettadpur, S., Watkins, M., and Reigber, C. (2004). The gravity recovery and climate experiment: Mission overview and early results. *Geophys. Res. Lett*, 31(9):L09607.

USGS (2011). centroid moment solution. `http://earthquake.usgs.gov/earthquakes/recenteqsww/Quakes/usc0001xgp.php`.

Wang, R. and Walter, T. (2011). Slip of the eurasian plate. `http://www.gfz-potsdam.de/portal/gfz/Public+Relations/M40-Bildarchiv/001_+Japan/110315_slip;jsessionid=7585960D2196612796EAEFDF675E73C3`.

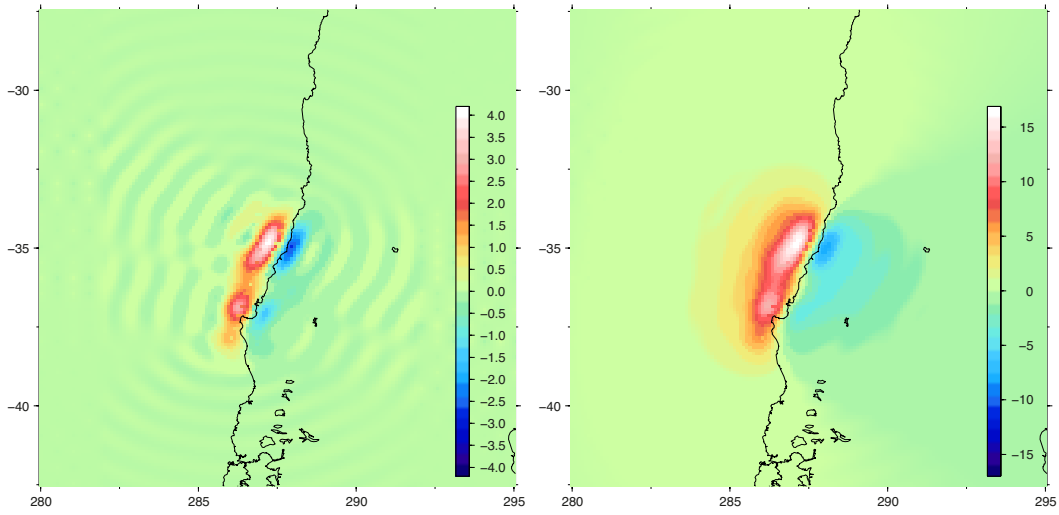

(a) vertical deformation, solid earth only (m)

(b) geoid height, solid earth only (mm)

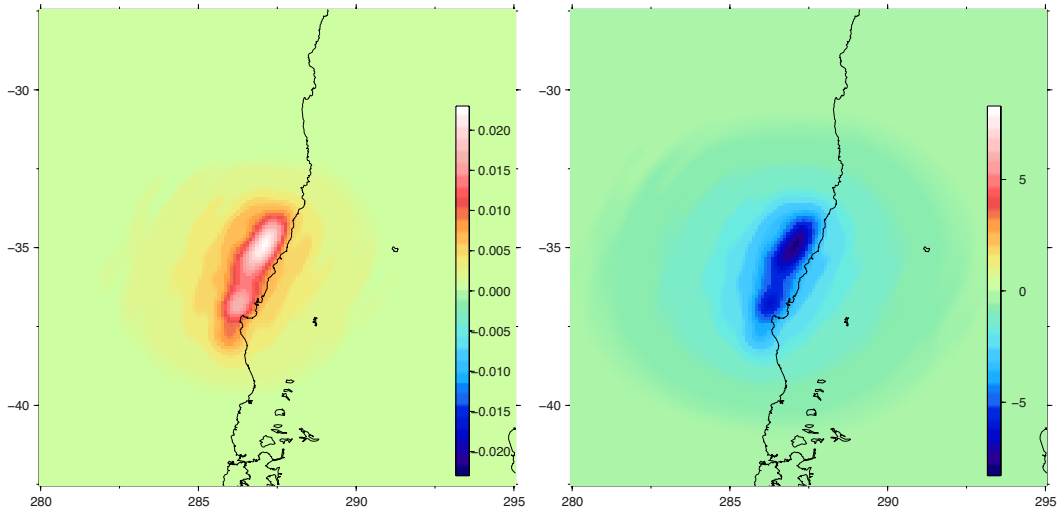

(c) vertical deformation, ocean effect (m)

(d) geoid height, ocean effect (mm)

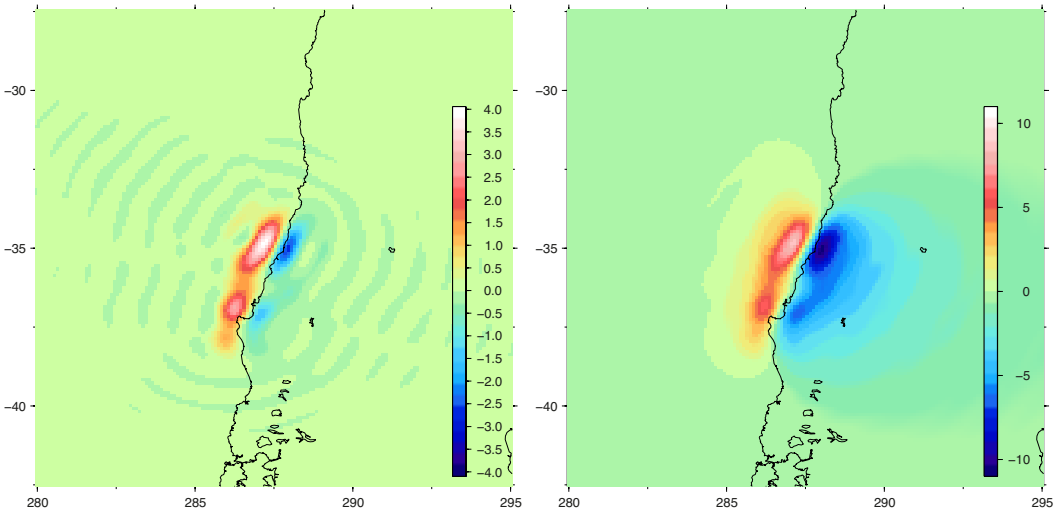

(e) vertical deformation total (m)

(f) geoid height total (mm)

Figure 3. Model results for the 8.8 Chile earthquake

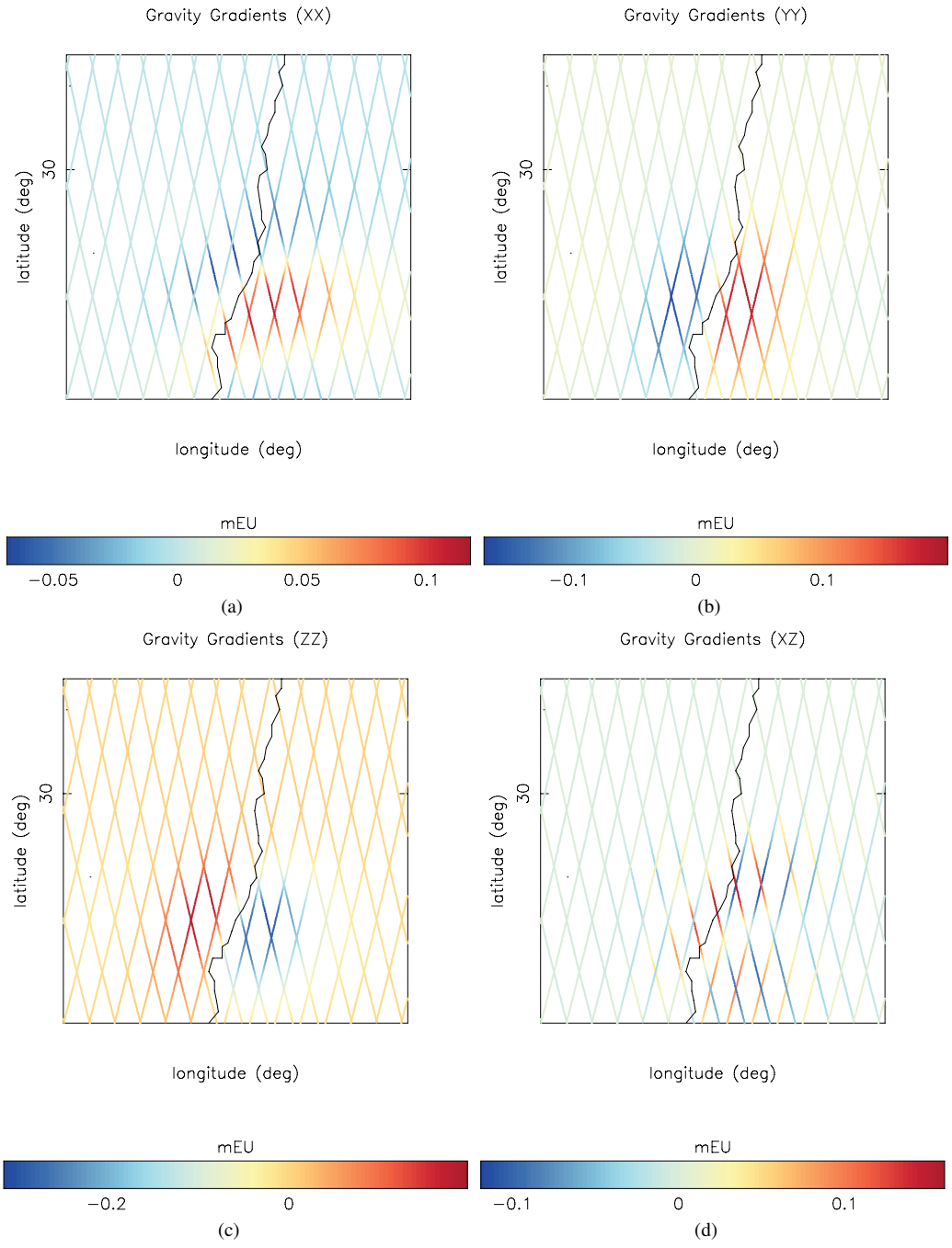

Figure 4. Modelled co-seismic gravity gradients along the GOCE orbit for the 8.8 Chile earthquake

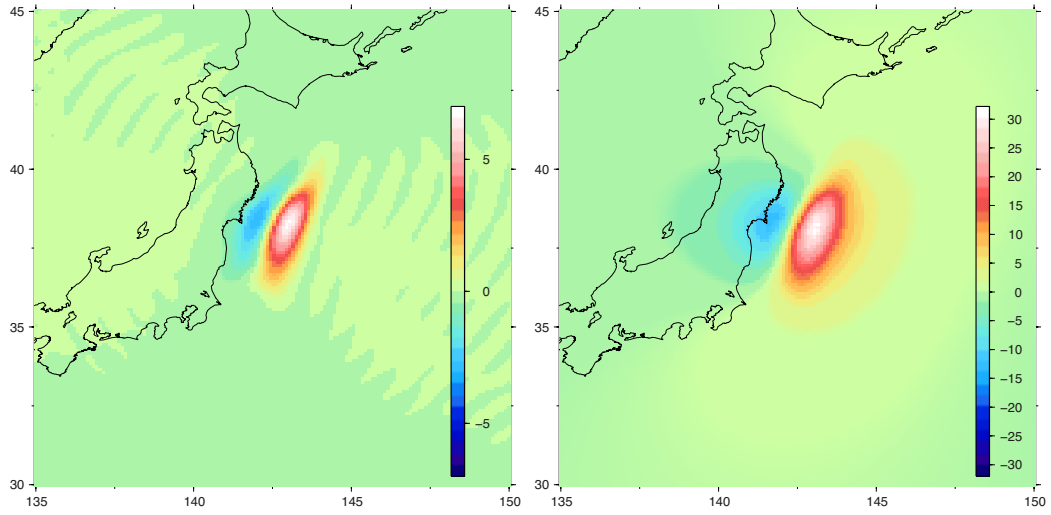

(a) vertical deformation, solid earth only (m)

(b) geoid height, solid earth only (mm)

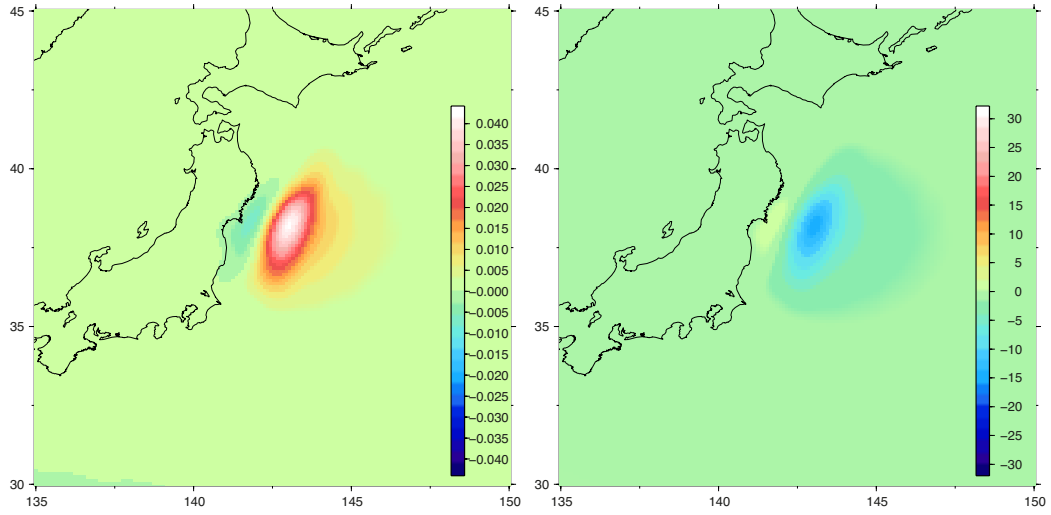

(c) vertical deformation, ocean effect (m)

(d) geoid height, ocean effect (mm)

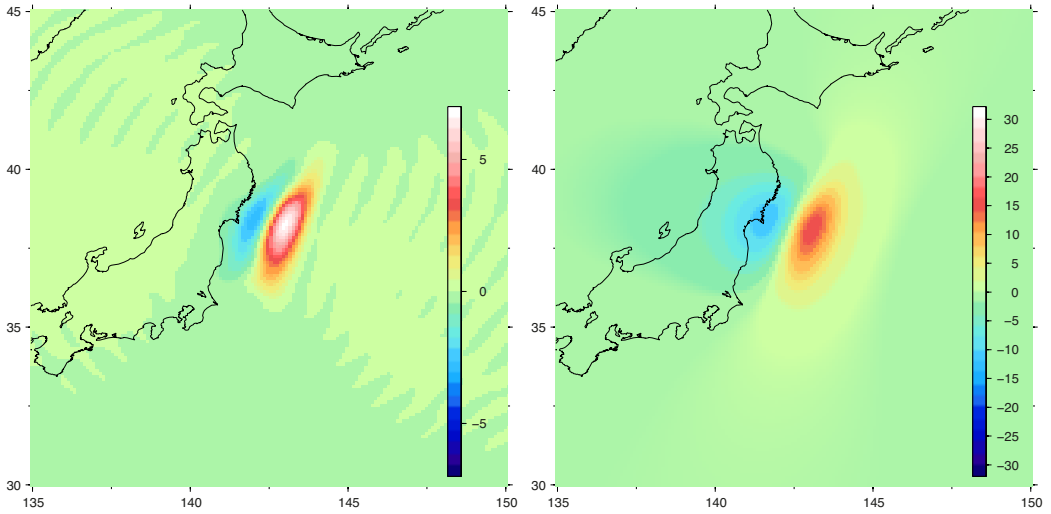

(e) vertical deformation total (m)

(f) geoid height total (mm)

Figure 5. Model results for the 9.0 Japan earthquake

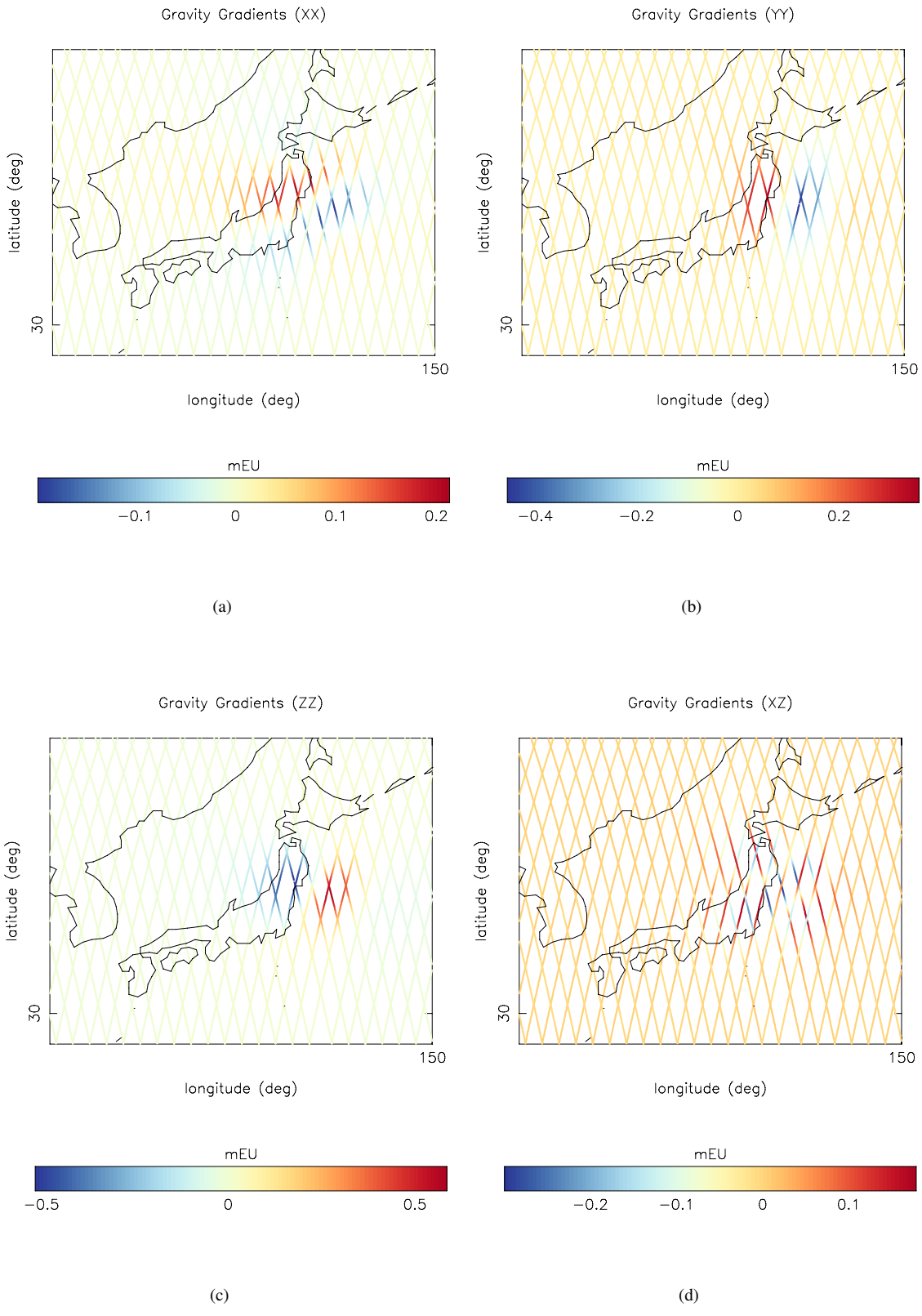

Figure 6. Modelled co-seismic gravity gradients along the GOCE orbit for the 9.0 Japan earthquake